



FEATURE EXTRACTION AND CLASSIFICATION OF GRAY-SCALE IMAGES OF BRAIN TUMOR USING DEEP LEARNING

KONDRA PRANITHA* AND NARESH VURUKONDA †

Abstract. Deep Learning using CNN plays a paramount role for the classification methods applied on medical image data. With a crucial role in accurate diagnosis, treatment planning and patient management for medical and healthcare systems, CNNs won accolades in the Deep Learning research. As simple the learning model so precise are the results for decision making. The proposed Sequential model of CNN is built with Parametric ReLU with the values aligned to geometric mean, attains a specific goal of tumor classification. The additional support of ground-truth aid in deciding the shape and severity of tumor in the Grayscale MRI of brain tumor. The simple Sequential model, although a minimal version has proved achieved significant classification goals using the GMP-ReLU. Comparative results with variants of ReLU have been charted in this article standing with the proof of consistent classification model with parametric-ReLU. The proposed design is conducted on images from Kaggle and a model is trained (classifier is built), which can be considered as ideal filter for all the benchmark images. The accuracy of proposed design is considerably improved compared to normal ReLU up to 89.214%

Key words: Deep learning, ground-truth based classification, parametric ReLU

1. Introduction. Brain is the most critical and vital organ in the human body. The root cause of dysfunction of the brain is the brain tumor. Excess of cells growing in the inter- and intra-circulatory regions of the brain causes lumps and muscular lesions called tumors. Tumors grow by consuming the nutrient inputs considered taking for the sake of body health. The tumors are located manually by expert clinicians and doctors in the human body using MRI images of the subjects, often causing inaccuracies and cumbersome in tracing, which takes more time. Brain cancer is caused by tumors which is critical and even causes death [1-3]. Therefore it shall be considered screened early in order to initiate remedial medicinal care and prevent well before growth of tumor is advanced. Classification helps in identifying the stages of the growth in tumors that cause deadly brain cancer [4-7]. Clinical diagnosis has more challenging issues related to tumor and cancer classification and identification. Medical Imaging introduces the medical image study methodology, where the experts can identify the crust of the tumors, edema or unorganized growths stemming in the inter-circulatory regions of the human body [8-10]. There are many imaging technologies invented since ages like computed tomography, positron emission tomography, magnetic resonance imaging and ultrasound. Even more complex imaging techniques were also developed to interact with the various sites of the human body[11]. Many medical institutions of various levels are applying the medical imaging technology which helps experts in visually diagnosing the internal regions anatomical and pathological strictures in the human body. Medical imaging protocols are developed envisioning the various types of diagnostic needs with different modalities of images.

The key stone in the gamut of mitigating with the patients affected with brain tumor is only early detection. Early detection reduces life and danger helps increased hope of survival possibilities. More than 90% of subjects recovered through early detection, whereas factor for not choosing is cost and availability of resources [12-14]. The best economic method would be detection and automation of image analysis through computer aided detection and diagnosis systems[15](CADDs).

The most popular method of imaging in the contemporary procedures is magnetic resonance imaging, which is more specifically used in diagnosis of brain cancer. As the brain cancer is arbitrary in size, location and affects type of the tumor, it is unpredictable for the conventional practitioners to guard on the eruption of cancer

*Department of Computer Science and Engineering, Koneru Lakshmaiah Education Foundation, Vaddeswaram, AP 522502, India (kondra.pranitha@gmail.com)

†Department of Computer Science and Engineering, Koneru Lakshmaiah Education Foundation, Vaddeswaram, AP 522502, India (naresh.vurukonda@kluniversity.in)

in the brain [16]. General metabolic flows in the brain are blocked by the tumors occurred by compressing the cells in the periphery of certain points which raises pressure, causing symptoms like nausea, imbalance walking and headache [17]. Such kind of inter-circulatory operations inside the brain cannot be traced with ultrasound or X-ray, where the malignity is location specific. Based on the examination required for the diagnosis, CT or MRI scanning is preferred to trace the foreign masses accurately. Most popularly used strategy for brain tumors is MRI which images the masses and the surroundings. Although, conventional procedures of MRI and CT support medical experts to review, as the MR images are high-definition images, rigid, non-ionizing and lasts considerably for longer time.

2. Literature Survey. Machine Learning has several steps to go through before an inference or knowledge is drawn from the data sets, such as: data augmentation, pre-processing, sampling, feature-detection, extraction, reduction and classification [18]. Feature extraction is the very important activity of the machine learning algorithms, in problems like classification, where the accuracy of the classification lies in extracting more positive features. Feature extraction considered as a low-level process, uses first-order statistics (like mean, median, standard deviation and skewness) are used in the low-level feature extraction [19-22]. Second order statistics such as shape, Gabor features and gray-level co-occurrence matrix were used to understand the formation of the foreign masses.

First order and second order statistics are employed for linear least square variant of support vector machine, which is used to develop the binary classifier, to classify malign or benign categories of brain MRI images [23]. Low-level features describe the tumor images efficiently, in spite of their representational efficiency due to similarity in appearances and anonymity of texture, shape and size, therefore gray level co-occurrence matrix (GLCM) [24-25] is applied for tumor identification and classification.

Hence, the traditional machine learning methods have problem in feature extraction stage, feature extraction need to be handcrafted based on the information available and methods applied, and there are more chances of human errors [26-27]. At this juncture, it is very essential to develop automated methods to refine the method of extraction of features using various types and levels of statistical information. An MRI image of brain has many mentions of details which are not in the texts and consensus of brain tumor literatures. In histopathology, experts can progressively identify and analyze certain impressions of features in MRI images [28-30]. Transformational reactions such as apoptosis and mitosis are not precisely studied in the conventional methods by the pathological experts, which prone to negligible errors, which even may cause morphologically a severe health menace. Histopathologists read certain features which has diagnostic leads, which are confined to limited subjectivity [31]. Other features which are found as peculiar and new to pathological analyses shall be extracted by data-driven approaches. A data-driven approach can grade the symptoms with considerable efforts of automated learning mechanism. ANN, SVM and Random Forests are allied methods that form into a conglomerate of analytical learning on the images, therefore the image analysis would pave into data driven learning and quantitative learning with salient pathological features.

Detecting the varying shape of the alien growth in the internal regions of the brain is not only relied on pattern recognition, where other non-structural properties also are influenced. For such situations, the parts that grow shall be examined as whether healthy or not. A brain atlas shall be studied for the various types of tissues in the internal regions of the brain, to assess the lesions are healthy or not. Symmetry of brain is also another important study where abnormal regions are detected that violates the symmetry.

During the study and classification of brain tumor, the reflections of the signals determine the type of tissue whether a tumor or not. The same signal intensities as that appear for a normal tissue appears for tumors which are categorized as isointense [27]. The isointense to hypo-intense properties of the tissues in the human brain associated with perilesional edema confuses the classification of brain tumor. Primary and secondary tumors such as meningioma (MEN), and metastasis (MET) respectively are detected using T1-weighted images of MRI for classification.

3. Brain Tumor Gray-scale MRI. One among the non-invasive techniques widely applied for diagnosis and monitoring of brain activities and tumors is MRI. Gray-scale MRI images provide valuable information about the tumor and surrounding tissue [13]. The resolution of these images can vary based on the acquisition protocol, imaging equipment, and specific clinical requirements. Some common resolutions for brain tumor gray-scale MRI images are:

Low resolution: Lower resolution images typically have a larger voxel size, which means each voxel represents a larger area in the scanned tissue. This can result in images with a resolution of around 256x256 or 128x128 pixels. While low-resolution images can be acquired quickly and require less computational resources for processing, they may lack the fine details needed for accurate diagnosis and treatment planning.

Medium resolution: Medium resolution images offer a balance between speed of acquisition and detail, with voxel sizes that are smaller than low-resolution images but larger than high-resolution images. These images often have resolutions around 512x512 pixels. Medium resolution images are commonly used in routine clinical practice, as they provide sufficient detail for most diagnostic purposes.

High resolution: High-resolution MRI images have small voxel sizes and capture finer details of the brain tissue, which can be crucial for certain applications, such as surgical planning or research. These images may have resolutions of 1024x1024 pixels or higher. High-resolution imaging can be time-consuming and require more advanced imaging equipment and computational resources for processing and analysis.

Super-resolution: Super-resolution is an advanced image processing technique that can be used to enhance the resolution of MRI images beyond the limits of the imaging equipment. Multiple image datasets with varied resolutions are combined from low-resolution images and super-resolution algorithms generate images with reasonable resolutions better comparable with high-resolution MRI. This can be particularly useful for applications where high-resolution images are needed but are difficult to acquire directly due to time or hardware constraints.

The choice of resolution for brain tumor gray-scale MRI images depends on the specific clinical scenario, diagnostic requirements, and available imaging equipment. In general, higher resolution images provide more detail and can potentially lead to more accurate diagnoses and treatment plans, but they also require more time to acquire and process.

4. Proposed Work. Brain tumor image analysis and segmentation is a subsidiary field of medical image analysis. From the research consensus in the recent decade, computer vision algorithms have profound contribution supporting diagnosis, treatment and monitoring the behavioral aspects of brain when affected by tumors. Much of the key features related to brain tumor such as size, location, type, grade, shape and boundaries, enhancing patterns, molecular features shall be understood during analyses shown in Fig.4.1.

4.1. Method of feature selection. Feature Selection has predominant role in classification and other prediction techniques. Feature selection is a preprocessing activity in deep learning for classification. Swarm based algorithms consists of two important characteristics which commonly prevail to demonstrate the meta-heuristic mechanism. Intensification and diversification are the two characteristics in swarm algorithms which do exploitation and exploration in the search space. Intensification aims at finding the best solution with respect to the current generation population in swarm optimization, whereas diversification is exploring the properties in the search space in stochastic orders, useful to evaluate the effectiveness of the algorithm. Most machine learning and deep learning algorithms employ meta-heuristic algorithms for feature selection. Meta-heuristic algorithms of swarm type are most suitable for the detection and identification of features in medical images. The phenomena of biological foraging behavior of animals, insects and sea-beings are most suitably applied for swarming in the feature selection of Fig.4.2.

4.2. Ground Truth images and their importance. The process of segmentation of brain tumor images from MRI is dynamic with respect to feature detection [46][51]. The process is vital in detecting features of tumors; delve in planning of treatment and to extract some findings different from healthy subjects. This is a challenging process, where varieties of methods are proposed in the research consensus. Manually rating the process of finding the standard validation in detecting the tumor features is always compared with the systematic or automated methods. The manual process of segmentation hinders with reliability, interpretation and reproducibility, more particularly at different regions employ different methods. Therefore, a ground truth needs to be prepared. a true ground truth is needed in segmentation of images manually. The importance of ground truth in detection and extraction of the known tumor features is more helpful. From the manual processes of segmentation of edema, several samples and estimates are considered to prepare the true ground truth.

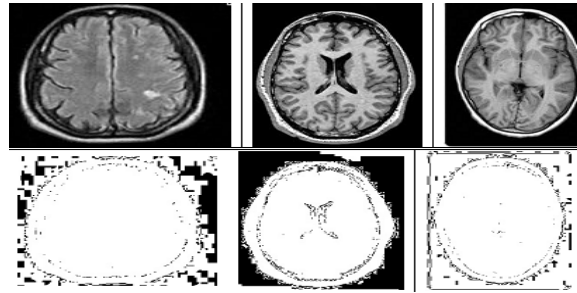


Fig. 4.1: Kaggle Images of Brain Tumors with ‘no tumor’ and the respective ground truths

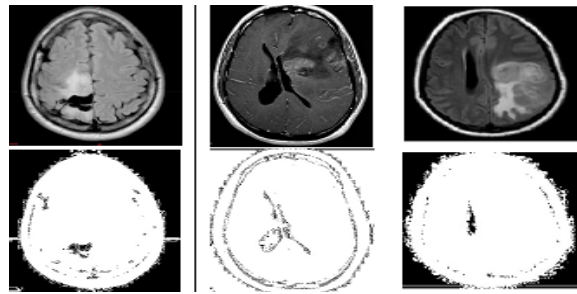


Fig. 4.2: Kaggle Images of Brain Tumors with ‘yes tumor’ and the respective ground truths

As the anatomy of brain tumor is complex, locating the points and positions of tumor requires intervention of experience of specialists. Characteristics of brain tumor and the detailed knowledge of brain functions and anatomy are essential for medical professionals including neurologists, oncologists and neuro-radiologists.

The following are the ground truth images of brain tumor data sets from Kaggle.

Ground truth images are annotated and labeled from the collective sources, where the reference information about the images is composed. Applied popularly in the deep learning techniques associated with classification, segmentation and object detection. Using ground truth, the performance of the algorithms can be evaluated with greater accuracy for the target sites in the medical images of brain tumor.

Ground truths for brain tumor images can be obtained by various methods such as manual segmentation, semi-automated segmentation, consensus labeling, synthetic or simulated data, which helps in developing and evaluating the performance of reliable computer vision algorithms.

4.3. Composition of CNN for selecting features using ground truths. The well-known fact about CNNs is it is a powerful class of deep learning model, which proves to be with exceptional performance particularly in computer vision research, such as segmentation, detection and recognition. When using CNNs for selecting features based on ground truths, the network is designed to learn meaningful representations from the input data, which can then be used for the given task. Here is a general outline for designing a CNN to select features using ground truths:

Input Layer: The raw image data sets are usually preprocessed and augmented considering the key parameters such as height, width and color channels and conversion into arrays.

Convolutional Layers: The building blocks of CNN, consists of various types of filters, kernels and striding mechanism performed through a convolution operation. Filters and kernels learn local features such as textures, corners and edges. **Activation functions:** At each convolution layer an activation takes place with a specific chosen function, to introduce the non-linearity, such as ReLU to substitute the equivalent values or chosen values for improvising the learnability.

Pooling Layers: Spatial dimensions of the images are converted to feature maps in pooling layers. The

computational complexity is reduced by overcoming the problems of overfitting. Max-pooling is the ideal process which considers the maximum values from a region in the feature map.

Fully connected layers: Feature maps in the form of arrays are flattened into a single vector after the pooling layer. Global features and relationships among different images are enabled to learn.

Output layer: The output layer is connected to the last fully connected layer and is responsible for producing the final feature vector or classification scores. Depending on the task, different activation functions are used, such as the softmax function for multi-class classification or sigmoid for binary classification.

Loss Function: The difference between the predictions and the ground truth labels are drawn, considering the cross-entropy loss during classification.

Optimization: An optimizer is used to revise the update the weights as per the learning requirements during training while minimizing the loss function.

Regularization techniques: To prevent overfitting and improve generalization, regularization techniques such as dropout, weight decay, or data augmentation can be applied. When designing a CNN for selecting features using ground truths, the network architecture, hyperparameters, and training strategy should be tailored to the specific task and dataset. This may require experimenting with different architectures, layer configurations, and learning rates to find the best combination that produces the most accurate and robust model.

4.4. Various Activation Functions used Feature Selection using Ground Truth. Activation functions play an essential role in Convolutional Neural Networks (CNNs) by introducing non-linearities that enable the network to learn complex patterns from the input data. There are several types of activation functions used in CNNs for feature selection based on ground truths. Some of the most common activation functions are: Rectified Linear Unit (ReLU): ReLU is the most widely used activation function in CNNs. It introduces non-linearity by setting all negative values in the input to zero, while keeping positive values unchanged. The simplicity of ReLU helps with faster training and reduced likelihood of vanishing gradients shown in Equ.4.1.

$$f(x) = \max(0, x) \quad (4.1)$$

Leaky Rectified Linear Unit (Leaky ReLU): Leaky ReLU is a modified version of the ReLU function that allows for a small, non-zero gradient when the input is negative. This helps to mitigate the "dying ReLU" problem, where some neurons become inactive and stop learning during training shown in Equ.4.2.

$$f(x) = \max(\alpha x, x) \quad (4.2)$$

where α is a small constant (e.g., 0.01)

Parametric Rectified Linear Unit (PReLU): PReLU is another variant of ReLU that generalizes Leaky ReLU by learning the slope of the function for negative input values during training. Equ.4.3 enables the model to adapt better to the specific characteristics of the dataset.

$$f(x) = \max(\alpha x, x), \quad (4.3)$$

where α is a learnable parameter

Exponential Linear Unit (ELU): ELU is an activation function that smooths the transition between positive and negative values by using an exponential curve. This smoothness helps to mitigate the vanishing gradient problem and speeds up training shown in Equ.4.4.

$$f(x) = x \text{ if } x \geq 0, \text{ else } \alpha(\exp(x) - 1) \quad (4.4)$$

Scaled Exponential Linear Unit (SELU): SELU is an activation function designed specifically for feed-forward neural networks with normalized weights and activations. When used with proper weight initialization and normalization, SELU can help the network to self-normalize, improving training stability and performance.

$$f(x) = \lambda x \text{ if } x > 0, \text{ else } \lambda \alpha(\exp(x) - 1) \quad (4.5)$$

In Equ.4.5, λ and α are predefined scaling factors

Table 5.1: Contrast Ratio

Contrast Ratio	RGB Values			Number of Images	Sample Size
	R	G	B		
	255	128 – 178	0 – 102	Total : 155	Avg. Size: 15
16	255	128	0	30	12
18	255	136	14	40	8
20	255	144	28	50	10
21	255	152	42	70	12
22	255	160	58	85	15
24	255	166	72	115	8
26	255	172	86	130	8
28	255	178	102	155	12

Hyperbolic Tangent (tanh): The tanh function is a scaled and shifted version of the sigmoid function that maps the input values to the range between -1 and 1. This activation function is less commonly used in CNNs due to the vanishing gradient problem, but can still be effective in certain cases shown in Equ.4.6.

$$f(x) = (exp(2x) - 1)/(exp(2x) + 1) \quad (4.6)$$

Sigmoid: The sigmoid function maps input values to the range between 0 and 1. While it is not commonly used as an activation function in hidden layers of CNNs due to the vanishing gradient problem, it is still useful in output layers for binary classification tasks.

$$f(x) = 1/(1 + exp(-x)) \quad (4.7)$$

Equ.4.7 gives the right activation function for a CNN depends on the specific task, dataset, and network architecture. In practice, ReLU and its variants (Leaky ReLU, PReLU) are the most popular choices due to their simplicity and effectiveness in most scenarios.

5. Results and Discussion. Synthetic samples of gray-scale brain tumor images are collected as input for the experimentation. The Kaggle data set is proposed with 253 images where 155 containing the symptoms of brain tumor and 98 images without any symptoms. The consideration of generating synthetic image data sets is to make the sample sizes bigger in order to provide larger scope for deep learning. Around 800 synthetic images are generated using Dezgo [www.dezgo.com], where the consistent availability of symptoms is unpredictable and suitable as an unknown input for the experiment. Most of the braintumor images drawn from the dataset contain pixels considering the hue values of 25 to 50, and saturation and luminosity values set up at constant 76% and 62% respectively in the regions notified as tumors. The regions look as blurry non-geometric areas which contain no crispy borders to locate the size and shape. Whether images contain features of tumor or not, it is very effortful to identify based on the colors, if color images are provided, therefore a Contrast Limited Adaptive Histogram Equalization method for the selected RGB density values of such areas are considered to supply as input the classification process to ascertain the presence of proliferative components. From the selected images containing suitable densities of pixels, as shown in the following table, a Sequential Model of CNN with kernel values as densities are iterated using various types of activation functions. The table shows number of images that arrive satisfactorily in the experiment for each activation function. Given with various levels of selected contrast ratios (drawn from the observations of the experiment), the range of R, G, B values are identified using RGB histograms (dcode.fr), for the images with tumor given in the Kaggle data sets. Number of images for each average sample size of 15 from the total number of images with tumor are noted in Table.5.1.

Typically an image histogram is a statistical graph, which represents the colors in the x-axis and distribution of RGB colors and Luminosity of image on the y-axis. A gross statistic of the image histogram represents a gray-scale version of luminosity and it is calculated for each pixel with the standard formula $0.2126 * R + 0.7152 * G + 0.0722 * B$.

Table 5.2: Classified Samples containing tumors with respect to implemented activation function

Description of Sample Selection (Contrast Ratio,Color after contrast)	No. of Images with tumor	Sample Size	Images in Classified Samples containing tumors with respect to implemented activation function				
			Sigmoid	Tanh	ReLU	Leaky ReLU	GMP-PReLU
Contrast Ratio : 16 Color : RGB(255, 128, 0)	30	12	8	9	8	7	10
Contrast Ratio : 21 Color : RGB(255, 152, 42)	60	12	10	10	9	8	11
Contrast Ratio : 22 Color : RGB(255, 160, 58)	65	15	8	10	8	7	12
Contrast Ratio : 26 Color : RGB(255, 172, 86)	70	8	5	8	6	5	7
Contrast Ratio : 28 Color : RGB(255, 178, 102)	75	12	8	10	8	7	12

The cloudy areas in the image represent tumor, the said color densities with contrast of 1% to 100% are considered in as a geometric progression shown in Table.5.2. The reason of using geometric progression in the experiment is the nature of the exponential spread style of the colored pixels. A pixel (p) is selected as a seed point of the random walk in the brain tumor image; the next pixel is detected with the same color with a distance(d). Thus, the infinite sum of the pixels is computed in geometric progression as in Equ.5.1.

$$\sum_{k=0}^{\infty} (p.d^k) = p \frac{1}{1-d} \tag{5.1}$$

For a sample window of the pixel values a series of contrast ratios accounted for the computation of the Geometric Progression sum, which may be considered as a parameter for the PReLU as first case in Table.5.3. Alternative case for Parametric ReLU is computed with value of α determined from a predefined value of pixel intensity with background knowledge, which is equivalent to the standard deviation of selected contrast ratios i.e., 16, 21, 22, 26, 28 is the value called ‘p’ which is replaced with α . The geometric progression of the min and max values of the selected contrast ratios of samples in an instance of observation is considered as an ideal value for the parameter shown in Table.5.4. Mean = 22.6, Sum of Contrast Ratios = 113 and Variance = 17.44

$$StandardDeviation(16, 21, 22, 26, 28) = \sqrt{1/N \cdot \sum_{i=1}^N (x_i - \mu)^2} = 4.1761226035642 \tag{5.2}$$

Margin of Error (Confidence Interval):

The distribution of the sampling mean is mostly as normal distribution. In this experiment, the standard error of the mean is computed as in Equ.5.3.

$$\sigma_x = \frac{\sigma}{\sqrt{numberofcontrastratio}} = 1.867618804 \tag{5.3}$$

Thus from the above observation of an instance of experimentation, the value of parameter ‘p’ is still corrected to $p = sd + sem$, where, if the confidence is considered as 95% of samples possess tumors $p1 = sd + sem$, for less than 95% samples $p2 = sd - sem$.

Table 5.3: Images in Classified Samples containing tumor with respect to implemented activation function GMP-PReLU

Description of Sample Selection (Contrast Ratio, Color after contrast)	No. of Images with tumor	Sample Size	Images in Classified Samples containing tumor with respect to implemented activation function GMP-PReLU		
			p1	p2	average
Contrast Ratio : 16 Color : RGB(255, 128, 0)	30	12	12	8	10
Contrast Ratio : 21 Color : RGB(255, 152, 42)	60	12	12	10	11
Contrast Ratio : 22 Color : RGB(255, 160, 58)	65	15	14	10	12
Contrast Ratio : 26 Color : RGB(255, 172, 86)	70	8	8	6	7
Contrast Ratio : 28 Color : RGB(255, 178, 102)	75	12	12	12	12

Table 5.4: Convolution Filters used in the Sequential Model of CNN

Layer(type)	Output shape	Param#
Conv2d(conv2D)	(None,30,30,32)	896
Max.Pooling2d(Max.pooling 2D)	(None,15,15,32)	0
Conv2d(Conv2D)	(None,13,13,64)	18496
Max.Pooling2d(Max.Pooling2D)	(None,6,6,64)	0
Conv2d(conv2D)	(None,4,4,64)	36928
Flatten(Faltten)	(None,1024)	0
Dense(dense)	(None,64)	656000
Dense(dense)	(None,10)	650

Detecting features is challenging as they are not found in specific spatial positions in the image. The convolution is performed on the various spatial areas of the image to determine whether it is a tumor Table.5.5.. In contrast to traditional neural network, the image has to transformed into a tensor rather into a vector in order to proceed with convolutions. A convolution filter is prepared, as a thumb rule with a size of 3x3 or 5x5. The following figure shows the 3x3 convolution filters:

The objective of the present application of Convolutional Neural Network is classification of the images with tumor from Kaggle repository in Table.5.6. The Keras Sequential API is primarily used and further up kept with modifications in convolution filters, ReLU and levels of layers.

```

model = models.Sequential()
model.add(layers.Conv2D(32, (3, 3), activation = 'relu', input_shape = (32, 32, 3)))
model.add(layers.MaxPooling2D((2, 2)))
model.add(layers.Conv2D(64, (3, 3), activation = 'relu'))
model.add(layers.MaxPooling2D((2, 2)))

```

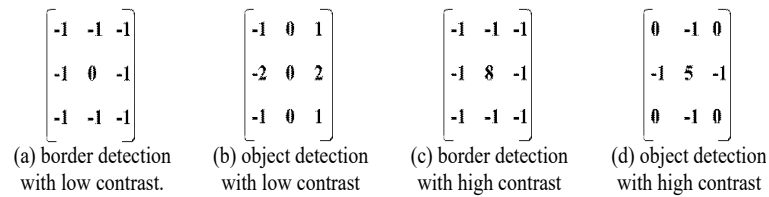


Fig. 5.1: Convolution Filters used in the Sequential Model of CNN

```
model.add(layers.Conv2D(64, (3, 3), activation = 'relu'))
```

The above lines of code are supported by a stack of 2D convolution layers and max pooling layers. The image input is prepared with parameters of width, height and the color channel irrespective of the batch size. A batch is the size / one chunk of input given to the Convolution Neural Network. The CNN processes the input with 32, 32, 3 as the width, height and the color channel respectively. The original size of the brain tumor images of the Kaggle datasets is 225 x 225, where a regular patch is extracted from the images of size 32x32x3. The first layer is given an input of a batch of size 16 images with 32x32x3 as input specifications. Tensors representing the width and height as dimensions of the images are the output from the convolution layer, where the images tend to shrink into deeper layers of the convolutional neural network model. The first argument controls the number of output of the channels (tentatively 32), as specifically width and height shrinks, more output channels are added to each convolution layer.

Tensor is the last output in the model, where it is fed into the convolution layer or into one or more dense layers, during classification, with the dimension of convolution as 4x4x64. As dense layers work on vectors, the tensors are converted into vectors, by means of flattening the tensor or unrolling the tensor, subsequently the dense layer is added at the top. The Kaggle datasets contains prospectively 2 to 4 classes; final dense layers of 2 or 4 in number are connected at the end of the convolutional network at 2 or 4 outputs. The following model summary demonstrate the CNN used in the experiment.

The network model proposed summarizes the model and the tensor (4, 4, 64) is flattened into vectors of shape (1024) with advanced application of two dense layers. Using adam optimizer of Keras and setting values of sparse categorical cross entropy in logit distribution the model is compiled and the accuracy and loss is traced in 10 epochs. The model is fit to the input and evaluated, for 10 epochs; the accuracy is obtained to 0.7192 and loss at 0.8475 with almost at average of 634 m/s per epoch. Further the model is evaluated for increasingly 15, 20, 50, 100, 150 epochs successively on the same inputs. The accuracy is obtained to 0.8792 and loss at 0.6432 with almost average of 714 m/s per epoch. In the proposed work, GMP-PReLU is implemented for better finding of images with dense clouds identified as tumors gray-scale images. The creation of GM-PReLU is a custom ReLU using Lambda layers in Tensorflow. An activation function can be created or edited using existing activation function. An example of implementation of custom ReLU is shown in the above code. The GMP-PReLU is introduced from standard samples of Kaggle data sets as cited previously. Selected samples of images containing severe features of tumors are considered and the pixel contrast ratio are computed. The pixel contrast ratios of the images are considered for the determination of the value of the 'p'.

As the parametric ReLU intervenes with an external input as a learnable parameter to regulate the learnability of ReLU, a value is computed consisting of characteristics of Geometric Mean, which improves the learning behavior in the classification model for Grayscale MRI of Brain tumor, exponentially compared with normal ReLU. Though, ReLU is the most popularly used activation function, which introduces non-linearity for all the negative values as zeroes, the linear identity of the positive values cannot draw suitable inferences of learning for all the images data with sparse information. Whereby, the activation function leads to null for most of the zero valued inputs in ReLU. To enhance such practical feasibility to overcome the flaws of learnability, Leaky ReLU can be worked out with the constant values of 0.01 or 0.001 for all the negatively assumed values in the sparse information of the image data sets. Whereas in the Parametric ReLU the constant values are instantaneously computed based on the population of gray-scale values for the image of the interest. Geometric

Table 5.5: Validation Parameters

Parameter	Computation
Accuracy	$\frac{TP+TN}{TP+TN+FP+FN}$
Error Rate	$\frac{FP+FN}{TP+TN+FP+FN}$
Positive Predict Value (PPV)	$\frac{TP}{TP+FP}$
Sensitivity	$\frac{TP}{TP+FN}$
Specificity	$\frac{TN}{TN+FP}$

Table 5.6: Classification with Sequential CNN using normal ReLU

No. of Samples	Observed Attempts		Cumulative Attempts		FPR	TPR	AUC
	Success	Fail	Success	Fail			
			0	0	1	1	0.074523
200	160	31	160	31	0.925477	0.972973	0.092901
250	205	36	365	67	0.829995	0.941587	0.105254
300	240	52	605	119	0.718211	0.896251	0.124398
350	298	57	903	176	0.579413	0.846556	0.139976
400	355	129	1258	305	0.414066	0.734089	0.11078
450	324	166	1582	471	0.263158	0.589364	0.071097
500	259	193	1841	664	0.142524	0.421099	0.034519
550	176	168	2017	832	0.06055	0.274629	0.010489
600	82	162	2099	994	0.022357	0.133391	0.002982
650	48	153	2147	1147	0	0	0
	2147	1147					0.76692

Mean of the trial values of positive values is calculated for the forthcoming values, if they are zeroes. The interpolative mechanism of employing values of Geometric Mean makes learning profitable. Deep Learning has ubiquitous methods for the problems of image classification, image annotation, image recognition and detection. The proposed model of CNN consists of 4 convolutional layers which are design with 16 feature maps. Thereby a Sequential Model of CNN could employ the ReLU with the said kind of parameters to avoid the saturation in learning. The feature maps after Max-Pooling is introduced with a kernel size of 2 x 2 and the normalization is directed by the normalization layers after each instance of Max-Pool layer, to enable faster convergence. Evaluating the performance of experiments is done by plotting the performance metrics of the observations in each instance of experiment. False Positive Rates and True Positive Rates are computed from all possible values of performance metrics and a curve is plotted. The curve between FPR and TPR denotes the gross variations of Sensitivity, Specificity and Accuracy achieved from the experiments. Wherefore, the experiments are conducted in two phases, that of a Sequential Model of CNN with normal characteristics of ReLU and GMPReLU, which is where the values obtained, are shown as ROC curve – Receiver Operating Characteristic curve. The following tables show tabulated data of the observations of the experiments of Sequential Model of CNN with ReLU and GMPReLU.

Evaluating the performance of experiments is done by plotting the performance metrics of the observations in each instance of experiment. False Positive Rates and True Positive Rates are computed from all possible values of performance metrics and a curve is plotted. The curve between FPR and TPR denotes the gross variations of Sensitivity, Specificity and Accuracy achieved from the experiments. Wherefore, the experiments are conducted in two phases, that of a Sequential Model of CNN with normal characteristics of ReLU and GMPReLU, which is where the values obtained, are shown as ROC curve – Receiver Operating Characteristic curve. The following tables show tabulated data of the observations of the experiments of Sequential Model of CNN with ReLU and GMPReLU.

The curve represents the performance of the experiments, where if the curve is closer to y-axis, the ex-

Table 5.7: Classification with Sequential CNN using GMP-ReLU

No. of Samples	Observed Attempts		Cumulative Attempts		FPR	TPR	AUC
	Success	Fail	Success	Fail			
			0	0	1	1	0.130485
200	226	4	226	4	0.869515	0.995859	0.152944
250	266	12	492	16	0.715935	0.983437	0.178291
300	314	14	806	30	0.534642	0.968944	0.186852
350	334	21	1140	51	0.341801	0.947205	0.211098
400	386	34	1526	85	0.118938	0.912008	0.036859
450	70	41	1596	126	0.078522	0.869565	0.032132
500	64	250	1660	376	0.04157	0.610766	0.014105
550	40	215	1700	591	0.018476	0.388199	0.005379
600	24	192	1724	783	0.004619	0.189441	0.000875
650	8	183	1732	966	0	0	0
	1732	966					0.94902

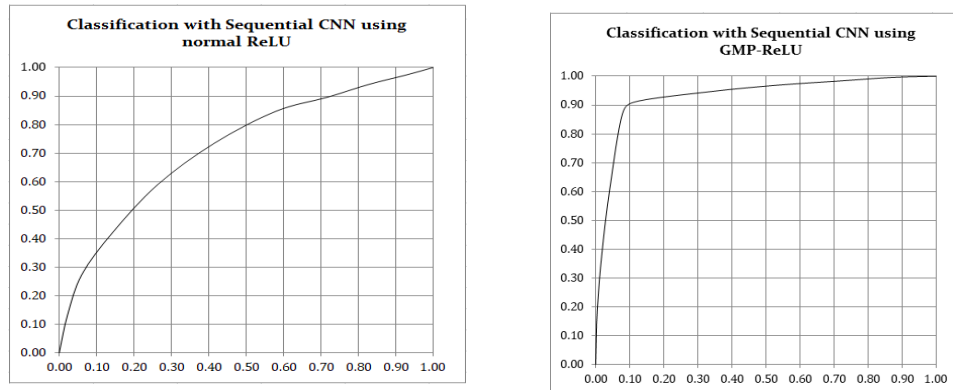


Fig. 5.2: The ROC showing the performance of the Sequential Model of CNN with ReLU and GMP-ReLU

periments exhibit a better fit. The AUC is also computed as the sum of values of product of the subsequent difference of FPR with the TPR is said to be achieved nearing to 1, indicating the maximum fit or better fit. Whereas, the value of AUC as 0.5 shows the indiscriminability of the model as success or failure of Table.5.7.

From observations of Fig.5.1, kernel shape and kernel size are progressively inverse. The reason is a very basic operational fundamental, as the kernel shape in first convolution passes, the resolution of the image is narrowed, in the sense the data is consolidated, thus by reducing size of kernel will increase proportionately. Number of convolutions is to narrow down the inferences obtained in the kernel, until a considerable inference is met; the convolutions are repeatedly performed. During the convolutions, the stride is considered to be 1 or 2, i.e., a unit matrix of one column and one row or a matrix with minimum countable columns and rows, which will be possibly 1 or 2. The stride indicates the number of kernel convolutions on the source image. Increase in the size of stride will reduce the resolution in the results as the number of convolutions becomes less in number.

As said above in the Sequential Model of CNN, application of filters means performing a convolution on the source. The size of the filter depends on the quality of comprehension required; size varies progressively in each iteration. The configuration of the framework consists of the pool size, stride size, computation on the pool, combining the results of computation from the convolutions by each filter. A filter is applied in convolutions on the source and completes all the computations of the source data, which is called as convolution layer. All the layers are combined into a tensor which is reshaped and flattened to a linear unit.

Ground truth based classification using convolution neural networks (CNNs) on gray scale images is a

common technique used in image recognition tasks. In this approach, a Sequential-CNN is trained using a data set of grayscale images that are labeled with the correct classes, known as the ground truth labels. The goal is to train the CNN to learn the features that are important for distinguishing between different classes of images. The process of training a CNN typically involves several steps, including data pre-processing, model design, and training. During the pre-processing step, the images are typically re sized and normalized to ensure that they are all the same size and have a consistent range of pixel values. This step is important for ensuring that the CNN can learn meaningful patterns from the images shown in Fig.5.2.

The model design step involves choosing the architecture of the CNN. Composition of multiple convolutional and pooling layers supporting convolution and pooling operations, which is typically followed by fully connected layers. The number and size of these layers will depend on the complexity of the problem being solved, and can be tuned through a process of experimentation and evaluation.

During the training phase, the labeled dataset is used in CNN for training, which is called backpropagation technique, where the weights are adjusted to minimize the variations among predicted labels and ground truth labels by the network. This process repeats as many epochs, or iterations, the network in the model achieve accuracy levels satisfactorily using training data.

A trained CNN for the specific input of training data sets can be conveniently used to classify new images of the training categories and at the final layer to determine the predicted class. Exclusive test data sets can be used to compare the performance of the network with predicted labels to the ground truth labels as a separate validation test.

6. Conclusion. In our experiment we have made an attempt to determine the tumor in Grayscale MRI of brain tumor. The training data is classified only for benign and malign. Meningioma as the primary and the metastases as secondary play rudimentary foal in the experiment. The synthetic data sets are used to build the training classifiers and then the training classifiers are applied on the real data sets in order to distinguish that with tumor or otherwise. Progressively, the iterations are performed in the experiment with varying sizes of kernel, in order to narrow the secondary tumors areas and improved resolutions of the inferences about primary tumors. The experiment is conducted on images from Kaggle and a model is trained (classifier is built), which can be considered as ideal filter for all the benchmark images. The accuracy of the model is considerably improved compared to normal ReLU up to 89.214%.

REFERENCES

- [1] Masood, Momina, Tahira Nazir, Marriam Nawaz, Awais Mehmood, Junaid Rashid, Hyuk-Yoon Kwon, Toqeer Mahmood, and Amir Hussain. "A novel deep learning method for recognition and classification of brain tumors from MRI images." *Diagnostics* 11, no. 5 (2021): 744.
- [2] Aggarwal, Ashwani Kumar. "Learning texture features from glcm for classification of brain tumor mri images using random forest classifier." *Transactions on Signal Processing* 18 (2022): 60-63.
- [3] Nawaz, Syed Ali, Dost Muhammad Khan, and Salman Qadri. "Brain tumor classification based on hybrid optimized multi-features analysis using magnetic resonance imaging dataset." *Applied Artificial Intelligence* 36, no. 1 (2022): 2031824.
- [4] Raza, Asaf, Huma Ayub, Javed Ali Khan, Ijaz Ahmad, Ahmed S. Salama, Yousef Ibrahim Daradkeh, Danish Javeed, Ateeq Ur Rehman, and Habib Hamam. "A hybrid deep learning-based approach for brain tumor classification." *Electronics* 11, no. 7 (2022): 1146.
- [5] Tummala, Sudhakar, Seifedine Kadry, Syed Ahmad Chan Bukhari, and Hafiz Tayyab Rauf. "Classification of Brain Tumor from Magnetic Resonance Imaging Using Vision Transformers Ensembling." *Current Oncology* 29, no. 10 (2022): 7498-7511.
- [6] Ahmed, Syed Thouheed, Vinoth Kumar, and JungYoon Kim. "AITel: eHealth Augmented Intelligence based Telemedicine Resource Recommendation Framework for IoT devices in Smart cities." *IEEE Internet of Things Journal* (2023).
- [7] Dhiman, Gaurav, V. Vinoth Kumar, Amandeep Kaur, and Ashutosh Sharma. "Don: deep learning and optimization-based framework for detection of novel coronavirus disease using x-ray images." *Interdisciplinary Sciences: Computational Life Sciences* 13 (2021): 260-272.
- [8] Babu, S. Sreedhar, and Polaiiah Bojja. "Abnormal Tumor Classification of MR Brain Images Using Deep Neural Networks." *Annals of the Romanian Society for Cell Biology* 25, no. 6 (2021): 4668-4680.
- [9] Guan, Yurong, Muhammad Aamir, Ziaur Rahman, Ammara Ali, Waheed Ahmed Abro, Zaheer Ahmed Dayo, Muhammad Shoaib Bhutta, and Zhihua Hu. "A framework for efficient brain tumor classification using MRI images." (2021).
- [10] Kang, Jaeyong, Zahid Ullah, and Jeonghwan Gwak. "MRI-based brain tumor classification using ensemble of deep features and machine learning classifiers." *Sensors* 21, no. 6 (2021): pp. 2222.
- [11] Irmak, Emrah. "Multi-classification of brain tumor MRI images using deep convolutional neural network with fully optimized

- framework." Iranian Journal of Science and Technology, Transactions of Electrical Engineering 45, no. 3 (2021): 1015-1036.
- [12] Khan, Hassan Ali, Wu Jue, Muhammad Mushtaq, and Muhammad Umer Mushtaq. "Brain tumor classification in MRI image using convolutional neural network." Mathematical Biosciences and Engineering (2021).
- [13] Badža, Milica M., and Marko Č. Barjaktarović. "Classification of brain tumors from MRI images using a convolutional neural network." Applied Sciences 10, no. 6 (2020): 1999.
- [14] Vinoth Kumar, V., V., Karthikeyan, T., Praveen Sundar, P. V., Magesh, G., & Balajee, J. M. "A quantum approach in life security using quantum key distribution." International Journal of Advanced Science and Technology 29 (2020): 2345-2354.
- [15] Gumaiei, Abdu, Mohammad Mehedi Hassan, Md Rafiul Hassan, Abdulhameed Alelaiwi, and Giancarlo Fortino. "A hybrid feature extraction method with regularized extreme learning machine for brain tumor classification." IEEE Access 7 (2019): 36266-36273.
- [16] Morad, Ameer Hussian, and Hadeel Moutaz Al-Dabbas. "Classification of brain tumor area for MRI images." In Journal of Physics: Conference Series, vol. 1660, no. 1, p. 012059. IOP Publishing, 2020.
- [17] NagaJyothi, Grande, and Sriadibhatla SriDevi. "Distributed arithmetic architectures for FIR filters-a comparative review." 2017 International conference on wireless communications, signal processing and networking (WiSPNET). IEEE, 2017.
- [18] Afshar, Parnian, Konstantinos N. Plataniotis, and Arash Mohammadi. "Capsule networks for brain tumor classification based on MRI images and coarse tumor boundaries." In ICASSP 2019-2019 IEEE international conference on acoustics, speech and signal processing (ICASSP), pp. 1368-1372. IEEE, 2019.
- [19] Das, Sunanda, OFM Riaz Rahman Aranya, and Nishat Nayla Labiba. "Brain tumor classification using convolutional neural network." In 2019 1st International Conference on Advances in Science, Engineering and Robotics Technology (ICASERT), pp. 1-5. IEEE, 2019.
- [20] Karthick Raghunath, K. M., Manjula Sanjay Koti, R. Sivakami, V. Vinoth Kumar, Grande NagaJyothi, and V. Muthukumar. "Utilization of IoT-assisted computational strategies in wireless sensor networks for smart infrastructure management." International Journal of System Assurance Engineering and Management (2022): 1-7.
- [21] Salçin, Kerem. "Detection and classification of brain tumours from MRI images using faster R-CNN." Tehnički glasnik 13, no. 4 (2019): 337-342.
- [22] Ari, Ali, and Davut Hanbay. "Deep learning based brain tumor classification and detection system." Turkish Journal of Electrical Engineering and Computer Sciences 26, no. 5 (2018): 2275-2286.
- [23] David, D. Stalin, and A. Jayachandran. "Robust classification of brain tumor in MRI images using salient structure descriptor and RBF kernel-SVM." TAGA Journal of Graphic Technology 14, no. 64 (2018): 718-737.
- [24] Vinoth Kumar, V., Karthikeyan, T., Praveen Sundar, P. V., Magesh, G., & Balajee, J. M. "Aspect based sentiment analysis and smart classification in uncertain feedback pool." International Journal of System Assurance Engineering and Management (2021): 1-11.
- [25] Seetha, J., and S. Selvakumar Raja. "Brain tumor classification using convolutional neural networks." Biomedical and Pharmacology Journal 11, no. 3 (2018): 1457.
- [26] Kumar, V. V., Raghunath, K. K., Rajesh, N., Venkatesan, M., Joseph, R. B., & Thillaiarasu, N. "Paddy plant disease recognition, risk analysis, and classification using deep convolution neuro-fuzzy network." Journal of Mobile Multimedia (2022): 325-348.
- [27] Abd-Ellah, Mahmoud Khaled, Ali Ismail Awad, Ashraf AM Khalaf, and Hesham FA Hamed. "Design and implementation of a computer-aided diagnosis system for brain tumor classification." In 2016 28th International Conference on Microelectronics (ICM), pp. 73-76. IEEE, 2016.
- [28] Belaid, Ouiza Nait, and Malik Loudini. "Classification of brain tumor by combination of pre-trained vgg16 cnn." Journal of Information Technology Management 12, no. 2 (2020): 13-25.
- [29] Bhanothu, Yakub, Anandhanarayanan Kamalakannan, and Govindaraj Rajamanickam. "Detection and classification of brain tumor in MRI images using deep convolutional network." In 2020 6th international conference on advanced computing and communication systems (ICACCS), pp. 248-252. IEEE, 2020.
- [30] Maithili, K., V. Vinothkumar, and P. Latha. "Analyzing the security mechanisms to prevent unauthorized access in cloud and network security." Journal of Computational and Theoretical Nanoscience 15.6-7 (2018): 2059-2063.
- [31] Zacharaki, Evangelia I., Sumei Wang, Sanjeev Chawla, Dong Soo Yoo, Ronald Wolf, Elias R. Melhem, and Christos Davatzikos. "MRI-based classification of brain tumor type and grade using SVM-RFE." In 2009 IEEE International Symposium on Biomedical Imaging: From Nano to Macro, pp. 1035-1038. IEEE, 2009.

Edited by: Polinpapilinho Katina

Special issue on: Scalable Dew Computing for Future Generation IoT systems

Received: Jul 28, 2023

Accepted: Nov 15, 2023